Journal of Optoelecrtonics and Advanced Materials, Vol. 4, No. 3, September 2002, p. 611 - 629

COMPOSITIONAL DEPENDENCE OF THE PHOTOINDUCED PHENOMENA IN THIN CHALCOGENIDE FILMS

K. Petkov

Central Laboratory of Photoprocesses, Bulgarian Academy of Sciences,
Acad. G. Bonchev Str., bil. 109, 1113 Sofia, Bulgaria

The results presented in this paper concern the changes in transmittance, reflectance, refractive index and band-gap in the visible and NIR region, transmissivity in the IR, dissolution rate in alkaline solutions and dry etching rate of some As- and Ge-containing chalcogenide thin films depending on composition and conditions of their deposition and exposure to light. It was found that the method of evaporation influences considerably the properties of thin chalcogenide films. The addition of Bi and Tl in As_2S_3 and GeS_2 leads to shifting of the absorption edge to the longer wavelengths. Using TRR_m methods (R_m is the reflection of 100 nm thick films deposited on Si substrate), the thickness of very thin layers from the systems As-S, GeS_2 and Ge-S-As have been determined with an accuracy of ±2 nm and for determination of the refractive index it was less than ±0.005. The data from the transmission measurements were compared with those from the ellipsometry. The great importance of evaporation temperature, film composition and pH of the solutions for achieving maximum change in the dissolution rate of the layers has been shown. It has been concluded that the irreversible changes resulting from illumination of as-deposited As-S films are connected with photo-induced transformation of the As-As and S-S bonds into As-S ones and subsequent polymerization of As_4S_4 molecules. The photo-induced changes in the ternary systems could be explained by the creation of new states in the band gap of the systems. These changes allow the practical application of thin-layered information recording media and high-resolution inorganic photoresists.

(Received July 11, 2002; accepted July 22, 2002)

Keywords: Chalcogenide glasses, Photo-induced effects, Inorganic photoresists

1. Introduction

The chalcogenide glasses are one of the most widely known families of amorphous materials and have been extensively studied for several decades because of their interesting fundamental properties and because of their potential applications in optical imaging, optical recording and integrated optics, microelectronics and optical communications. Most of these applications are based on the wide variety of light-induced effects exhibited by these materials [1-5]. These photo-induced phenomena have been studied in many laboratories for many years and many review papers have already been published [6-9]. The determination of the optical constants is of great importance for understanding the mechanism of the optical processing and for their application in practice. A number of works exist which trace the influence of composition and preparation conditions of thin films on the physico-chemical properties, and the changes in them induced by light. The structural changes in these materials are related to the changes in their optical properties.

Various methods exist for determining the optical constants of thin films from the coefficient of transmission, T, and reflection, R, or via their combination [10-15]. All these methods are based on the Swanepoel's method [16] and on different computer programs for calculation of the optical constants and film thickness. As the layer structure depends strongly on the conditions of the film

deposition it is difficult to make some comparison between the published data in the literature.

In this paper, a review of the results from the research done in the Central Laboratory of Photoprocesses of the Bulgarian Academy of Sciences on the photoinduced changes in dissolution rate, optical properties and structure of thin chalcogenide films from the systems As-S, As-S-Ge, As-S-Bi(Tl) and Ge-S-Bi(Tl) aimed at creation of photoresist systems and optical recording media is presented.

2. Experimental

The investigations were made on chalcogenide thin films of the systems As_xS_{100-x} ($28 \leq x \leq 45$), $(As_2S_3)_{100-x}Me_x$ ($0 \leq x \leq 10$), $Ge_xAs_{40-x}S_{60}$ ($0 \leq x \leq 40$) and $(GeS_2)_{100-x}Me_x$ ($0 \leq x \leq 10$) where Me = Bi, In or Tl. The initial substances were prepared by melting calculated quantities of As, Ge, S, Bi, In and Tl, [17, 18, 19] with a purity higher than 99,999%, in a quartz ampoule welded in a vacuum of 10^{-3} Pa. After evacuating the residual gases it was placed in the oven where melting of the components took place at temperatures around 700 °C for 10 hours (As-S glasses), 870 °C – 12 hours (As-containing glasses) and 970 °C for 36 hours (Ge-containing glasses). In order to achieve good homogenization of the chalcogenide glasses and to produce glass with uniform composition, the oven is slowly rocked during the time when the ampoule is at high temperature. The composition of the bulk glasses as well as of the thin films was determined in a scanning electron microscope with X-ray microanalyzer (Jeol Superprobe 733, Japan) [20, 21]. Table 1 shows the mean data for the element content in a selection of the bulk glasses, including some of those exhibiting the greatest changes in the optical properties, as will be shown further below. It is evident from the table that the compositions of the bulks are generally within ~1 at.% of the expected compositions. The bulk samples were subjected to diffraction analysis, which confirmed that only amorphous phase was identified except composition $As_{45}S_{55}$ (with traces of crystalline phase) and Ge-S-Tl glasses (with small crystalline α-GeS_2 phase).

Thin films were deposited at room temperature onto optical glass substrates BK-7, Si wafers and graphite substrates by thermal evaporation from a molybdenum crucible under a vacuum of $6\text{-}8.10^{-4}$ Pa. The deposition rate was controlled by the change of the intrinsic frequency of oscillation of a piezocrystal and was ~ 0.5 nm/s. The element content of the films obtained by different deposition methods was determined using samples deposited on graphite (Table 1). The element content strongly depends on the conditions of the ternary film deposition.

Table 1. Mean data for the element content for some of the bulk and thin film chalcogenide samples.

Composition	Nominal composition (at.%)	Obtained composition (at.%)	
		Bulk glass	Thin film
As_2S_3	$As_{40}S_{60}$	$As_{39}S_{61}$	$As_{40}S_{60}$
As_2S_4	$As_{33}S_{67}$	$As_{34}S_{66}$	$As_{33}S_{67}$
As_2S_5	$As_{28}S_{72}$	$As_{29}S_{71}$	$As_{28}S_{72}$
$As_{42}S_{58}$	$As_{42}S_{58}$	$As_{43}S_{57}$	$As_{42}S_{58}$
$(As_2S_3)_{94}Bi_6$	$As_{38}S_{56}Bi_6$	$As_{39}S_{35}Bi_6$	$As_{44}S_{51}Bi_5$
$(As_2S_3)_{94}Tl_6$	$As_{38}S_{56}Tl_6$	$As_{37}S_{67}l_6$	$As_{42}S_{54}Tl_5$
$Ge_{20}As_{20}S_{60}$	$Ge_{20}As_{20}S_{60}$	$Ge_{21}As_{19}S_{60}$	$Ge_{21}As_{19}S_{60}$
$Ge_{20}S_{80}$	$Ge_{20}S_{80}$	$Ge_{25}S_{75}$	$Ge_{23}S_{77}$
$Ge_{33}S_{67}$	$Ge_{33}S_{67}$	$Ge_{33}S_{67}$	$Ge_{35}S_{65}$
$Ge_{40}S_{60}$	$Ge_{40}S_{60}$	$Ge_{40}S_{60}$	$Ge_{39}S_{61}$
$(GeS_2)_{94}Bi_6$	$Ge_{31}S_{63}Bi_6$	$Ge_{28}S_{66}Bi_6$	$Ge_{31}S_{66}Bi_3$
$(GeS_2)_{94}Tl_6$	$Ge_{31}S_{63}Tl_6$	$Ge_{31}S_{63}Tl_6$	$Ge_{32}S_{61}Tl_7$
$(GeS_2)_{94}In_6$	$Ge_{31}S_{63}In_6$	$Ge_{35}S_{58}In_7$	$Ge_{35}S_{60}In_5$

Optical transmission measurements were made using a UV/VIS/NIR spectrophotometer (CARY 05E, USA) to an accuracy better than ±0.1%, and the absolute reflection, R, was measured with VW accessories - better than ±0.5% in the spectral range 350 to 1500 nm. The ellipsometric measurements were carried out at three angles of incidence of light (45, 48 and 50 °), at λ = 632.8 nm, using MAI-ellipsometry. The illumination of thin films was realized by a halogen lamp (20 $mW.cm^{-2}$) in air. The exposure time to saturation (i.e. the time beyond which the absorption edge did not change) was experimentally established for all compositions. The structure of the layers was investigated by Scanning Electron Microscopy (SEM) and Transmission Electron Microscopy (TEM) (Philips, Netherlands).

The refractive index, n, and the film thickness were calculated using Swanepoel's method [16] and a computer program developed by Konstantinov [22]. The method allows the calculation of n when both the refractive index of the substrate and the position of the interference extrema are known. In the present study the refractive index, s, of the substrate was determined independently at various wavelengths by measuring the transmittance, T_s, of the substrate alone and using the equation [22]:

$$s = 1/T_s + 1/(T_s^2 - 1)^{1/2}. \quad (1)$$

For BK-7 glass substrate it was found that $91 \le T_s \le 92$ and $89 \le T_s \le 91$ over the wavelength ranges 350-1400 nm and 1400-2500 nm, respectively. The program used to calculate n will determine it to an accuracy of ±0.5 % for an error in the transmittance of ±0.1 %.

For chalcogenide semiconductors, the optical absorption coefficient, α, changes rapidly for photon energies comparable to that of the band-gap, E_g, giving rise to an absorption edge with three regions – for the largest electron energies, in the region of the edge itself ($10 < \alpha < 10^4$ cm^{-1}) and at the lowest photon energies [5]. The first one is for the highest values of the absorption coefficient ($\alpha \ge 10^4$ cm^{-1}) which corresponds to transitions between extended states in both valence and conduction bands where the power law of Tauc [23]

$$\alpha h\nu = B(h\nu - E_g)^2 \quad (2)$$

is valid. B is the slope of the Tauc edge which reflects some disorder of the samples. Usually this constant depends on the width of the localized states in the band-gap, a fact explained with the homopolar bonds in the chalcogenide glasses. Thus, Tauc plots of $(\alpha h\nu)^{1/2}$ *versus* ($h\nu$) should be linear and extrapolate to values of the optical gap, E_g.

In the third region, the absorption coefficient presents exhibits an exponential behaviour

$$\alpha = \alpha_0 \exp(h\nu)/E_e. \quad (3)$$

The absorption in this region is due to transitions between extended states in one band and localized states in the exponential tail of the other band. E_e is connected with the width of the more extended band tail and it is often called the Urbach energy. It is determined by the degree of disorder in the amorphous chalcogenides.

The thickness to an accuracy of ±1-2 nm and the optical constants of chalcogenide films (100 nm thick) were determined by two triple (T, R_f, R_m) and (T, R_b, R_m) methods [24, 25]. The subscripts f and b denote the light reflection from the film side and from the substrate (BK-7) side, respectively, while m represents the reflection of the same film deposited on a Si wafer. The most accurately calculated film thicknesses were used for the determination of the optical constants by double (T, R_f) and (T, R_b) methods, using the Newon-Raphson's interative method [26]. For each of the applied methods for determining the optical constants and thickness, the absolute maximum errors were evaluated [27]. From the relationship $d = f(\lambda) = const$, obtained by the triple methods, the physically corrected solutions for d were isolated.

The kinetics of thin films dissolution was studied by a method based on the change in the intensity of weakly absorbing light from He-Ne laser (λ = 632.8 nm) during film dissolution [28]. The solvents used were aqueous solutions of dimethylamine, NaOH, K_2CO_3, Na_2CO_3 and Na_3PO_4 with or

without surfactants, with pH = 10.5-12.5. The pH values were adjusted by adding Na_3PO_4 and were measured with a G-14 electrode using a GTE pH-meter (Seibold, Austria).

The XPS studies were carried out in an Escalab MkII electron spectrophotometer (VG Scientific) with base pressures in the preparation and analysis chambers of 2.10^{-8} and 1.10^{-8} Pa, respectively. The photoelectrons were excited using an X-ray source (Mg Kα , 1253.6 eV). At an analyser pass energy of 20 eV, the instrumental resolution measured as the full width at half-maximum (FWHM) of the Ag 3d5/2 photoelectron peak was 1.2 eV. The binding reference energy of Au 4f7/2 was assumed to be 83.8 eV. This allowed determination of binding energy of the As 3d, S 2p and O 1s peaks with an accuracy of ± 0.1 eV [29].

3. Results

3.1. Optical properties of thin As-S and As-S-Ge films

The properties of the system As-S as one of the glass-forming systems are extensively studied and data for the absorption coefficient, the band-gap and the refraction index of thin films and their changes after illumination exist in the literature [10, 11]. In our experiments thin As_xS_{100-x} ($28 \le x \le 45$) and $As_{40-x}Ge_xS_{60}$ ($0 \le x \le 40$) films were deposited by thermal evaporation with a deposition rate 1.0-1.5 nm/s and the optical constants were calculated. The different conditions of evaporation included different rates of deposition of pre-weighted quantities of glasses for obtaining the thickness which was necessary and the case when the evaporation process was stopped when the film thickness was about 1000 nm with a residue in the boat. The refractive index and thickness were calculated from the transmission spectra according to [16, 22] and using double and triple methods for calculation of the optical constants [24, 25]. For determination of the optical homogeneity of the thin films some experiments on thin layers (about 80 nm thick) deposited consecutively in the same vacuum cycle and a layer which thickness represents a sum from their thicknesses have been done. Table 2 shows the experimental data for the shift of the absorption edge, $\Delta\lambda$, the refractive index n for unexposed and exposed films (1.0 µm and 80 nm thick), and Δd from transmission and ellipsometric measurements of thin As_xS_{100-x} ($28 \le x \le 45$).

Table 2. Experimental values of $\Delta\lambda$, n (at λ = 632.8 nm), Δd and E_g for unexposed and exposed thin As-S films, deposited with a residue in the boat (1 – 1000 nm and 2-100 nm thick films).

Composition	Δλ [nm] (T=20 %]	n unexp (1)	n exp (1)	Δn (1)	n unexp (2)	n exp (2)	ΔE_g (eV)	Δd [nm]
$As_{28}S_{72}$	+ 4	2.33	2.40	0.07	2.33	2.41	2.53	-15
$As_{32}S_{68}$	+ 5	2.43	2.50	0.07	2.42	2.47	2.45	-11
$As_{40}S_{60}$	+10	2.44	2.56	0.12	2.46	2.55	2.38	-8
$As_{45}S_{55}$	+9	2.43	2.52	0.09	2.45	2.54	2.36	-9

The calculated values of the refractive index of unexposed thin As_xS_{100-x} films ($28 \le x \le 45$) are in a good agreement with the results published in the literature [10, 30, 31]. The refractive index as well as the absorption edge shift increase with increasing of the As content in the films and pass through a maximum for the stoichiometric composition $As_{40}S_{60}$. After exposure to light, n and the compactness of the layers increase (for $As_{40}S_{60}$ - Δn = 0.12 at λ = 632.8 nm and Δd = 8 nm). The same dependence for n, d and Δλ was observed when the calculation was made from the ellipsometric measurements and using double and triple spectroscopic methods. The thickness of the layers does not influence the optical properties of the As-S coatings and the ellipsometric measurements under different angles of incidence of the light show that all As-S films are homogeneous in thickness.

The absorption coefficient, α, calculated from (1) shows a linear dependence in the region of high adsorption. The band-gap determined from the plots $(\alpha h\nu)^{1/2}$ vs. ($h\nu$) decreased with increasing the As content in the films (from 2.53 eV for $As_{28}S_{72}$ to 2.36 eV for $As_{45}S_{55}$). For S enriched thin films

the quantity of S-S bonds, which are longer than As-S and As-As ones, increase. That leads to an increase of the average length and to an increase in the band-gap. After illumination E_g decreases for all the composition investigated and the factor B increases (for example - from 795 $cm^{-1/2}eV^{-1/2}$ for as-deposited $As_{40}S_{60}$ to 876 $cm^{-1/2}eV^{-1/2}$ – for the exposed). According to Mott and Davis [32] the changes in B could be connected with the creation of the localized states in the band-gap.

In Fig. 1 the plots of the optical transmission as well as the dispersion of the refractive index of thin GeS_2 and As-S-Ge films versus wavelength, before and after exposure to light are presented. The compositions are the ones exhibiting the largest light-induced changes in the optical properties. It was found that after illumination the absorption edge shifts to the shorter wavelengths (an effect of photobleaching) and the highest shift in the absorption edge ($\Delta\lambda$ = -30 % at T = 20%) and the refractive index (Δn = - 0.07) belong to the composition $As_{10}Ge_{30}S_{60}$. When Ge content increases the changes in the optical properties decrease.

Table 3 shows the main data for the thickness of thin As-Ge-S films determined by UV-VIS-NIR spectrophotometry using T, R, R_m method and by ellipsometry. It seems that there is no difference in the thickness values of thin films from the investigated system.

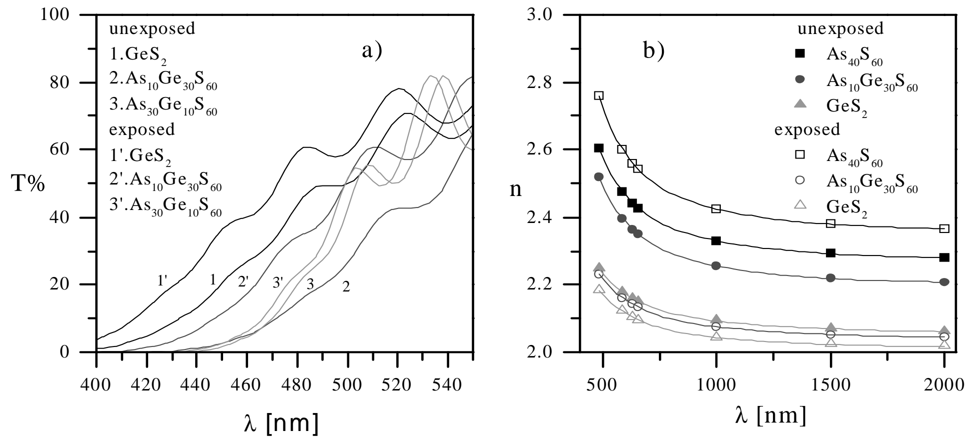

Fig.1. Optical transmission (a) and refractive index dispersion (b) of thin As-S-Ge films vs. wavelength, λ, before and after illumination. These compositions are the ones exhibiting the largest light-induced changes in optical properties.

Table 3. Data for the thickness of thin As-Ge-S films determined by UV-VIS-NIR spectrophotometry using a T, R, R_m method and by ellipsometry.

Composition	(T, R, Rm) method		Ellipsometric	
	d $_{unexp}$ [nm]	d $_{exp}$ [nm]	d $_{unexp}$ [nm]	d $_{exp}$ [nm]
As_2S_3	70 ± 1.0	68 ± 1.0	69.4 ± 0.1	69.5 ± 0.2
$As_{30}Ge_{10}S_{60}$	95 ± 1.5	91 ± 2.0	93.6 ± 0.2	91.5 ± 0.1
$As_{20}Ge_{20}S_{60}$	80 ± 1.0	85 ± .1.3	81.8 ± 0.2	86.2 ± 0.2
$As_{10}Ge_{30}S_{60}$	52 ± 1.0	57 ± 1.0	53.6 ± 0.2	57.7 ± 0.3
GeS_2	48 ± 1.5	50 ± 1.0	47.0 ± 0.2	49.7 ± 0.2

The optical constants determined by UV-VIS-NIR spectrophotometry depending on the film composition were compared with the data obtained on the same samples by MAI-ellipsometry (Table 4).

After exposure of thin As-S-Ge layers to light to saturation n decreases and the thickness increases. The highest change in n was observed for $As_{10}Ge_{30}S_{60}$ layers (Δn = - 0.07) (Fig. 1b). The same dependence of $n = f(\lambda)$ for unexposed and exposed thin As-Ge-S films was observed when (T, R_f) and (T, R_b) methods were used (Table 4).

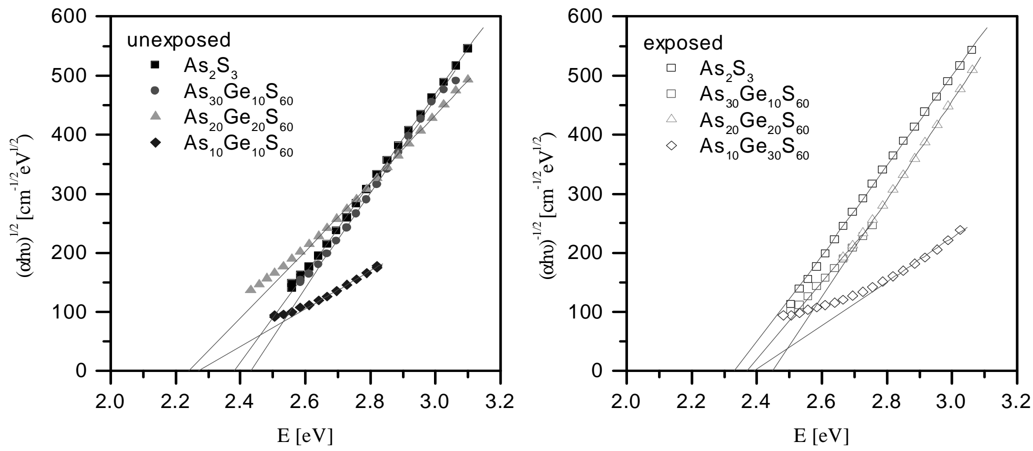

Fig. 2. Optical absorption edge ($\alpha h\nu$)1/2 vs. photon energy ($h\nu$) for unexposed and exposed thin As-S-Ge films.

The calculated values of the absorption coefficient, k , from the above mentioned methods were used for calculation of the absorption coefficient α ($\alpha = 4\pi k/\lambda$). Fig. 2 shows the plots of the $(\alpha h\nu)^{1/2} = f(h\nu)$ dependence. When Ge was added to As_2S_3 the optical band gap, E_g, increases for the unexposed layers. After exposure to light E_g increases and the biggest change $\Delta E_g = 0.21$ eV was observed for thin film with composition $As_{20}Ge_{20}S_{60}$ (Table 5). The results for the composition dependence and the influence of the light obtained by refractive ellipsometry were in a good agreement with the data from the transmission spectrophotometry. It was found that $k = 0$ when the optical constants were determined at 3 different angles of incidence of light on the sample and the calculated values of n at 45, 48 and 50° show that both unexposed and exposed thin As-Ge-S films are homogeneous.

Table 4. Data for the refractive index of thin As-Ge-S films with thickness of 1000 nm and below 100nm at $\lambda = 632.8$ nm obtained by UV - VIS - NIR spectrophotometry (1) and by ellipsometry (2).

Composition	Thin films 1000 nm thick				Thin films about 100 nm thick			
	Unexposed		Exposed		Unexposed		Exposed	
	1	2	1	2	1	2	1	2
As_2S_3	2.44	2.458	2.56	2.531	2.46	2.490	2.55	2.581
$As_{28}S_{72}$	2.33	2.428	2.40	2.417	2.33	2.414	2.42	2.456
$As_{33}S_{67}$	2.43	2.422	2.50	2.441	2.42	2.450	2.47	2.520
$As_{45}S_{55}$	2.43	2.456	2.52	2.553	2.45	2.454	2.54	2.553
$As_{10}Ge_{30}S_{60}$	2.32	2.336	2.23	2.258	2.34	2.327	2.12	2.201
$As_{20}Ge_{20}S_{60}$	2.35	2.369	2.30	2.280	2.34	2.388	2.23	2.281
$As_{30}Ge_{10}S_{60}$	2.45	2.431	2.44	2.415	2.46	2.556	2.46	2.552
GeS_2	2.15	2.131	2.11	2.096	2.12	2.131	2.02	2.027

The values of n, $\Delta\lambda$ and E_g determined for the As-S-Ge system are in a good agreement with other published data [22, 33] where the maximum changes in the optical properties are observed for the composition $As_{20}Ge_{20}S_{60}$. The assumption of Tanaka [34] that for ternary As-S-Ge system, the photo-induced structural changes are mostly expressed for compositions with the coordination value $z = 2.6$-2.7 is confirmed.

Table 5. Data for the optical band gap of unexposed and exposed thin As-Ge-S films.

Composition	$E_{g\ unexp.}$ [eV]	$E_{g\ exp.}$ [eV]	ΔE_g [eV]
As_2S_3	2.38	2.33	-0.05
$As_{30}Ge_{10}S_{60}$	2.42	2.49	+0.07
$As_{20}Ge_{20}S_{60}$	2.24	2.45	+0.21
$As_{10}Ge_{30}S_{60}$	2.27	2.39	+0.12
GeS_2	2.53		

3.2. Optical properties of thin As-S-Bi(Tl) films

Thin films (1000 nm thick) from the system As-S-Bi(Tl) were deposited by thermal evaporation of bulks with compositions $As_{39}S_{58}Bi_3$, $As_{38}S_{56}Bi_6$, $As_{36}S_{54}Bi_{10}$, $As_{39}S_{58}Tl_3$, $As_{38}S_{56}Tl_6$ and $As_{36}S_5Tl_{10}$ [35]. It was found that the absorption edge of unexposed thin layers was shifted to longer wavelengths increasing the Bi or Tl content in As_2S_3 (Fig. 3a). After exposure to light an effect of photobleaching occured. The largest value of the shift of the absorption edge, $\Delta\lambda$, was observed for thin films with compositions $As_{39}S_{58}Bi_3$ ($\Delta\lambda$ = +15 nm at T = 20%) and $As_{38}S_{56}Tl_6$ ($\Delta\lambda$ = +26 nm at T = 20%). An increase in the Bi or Tl content leads to decreasing in the shift of the absorption edge.

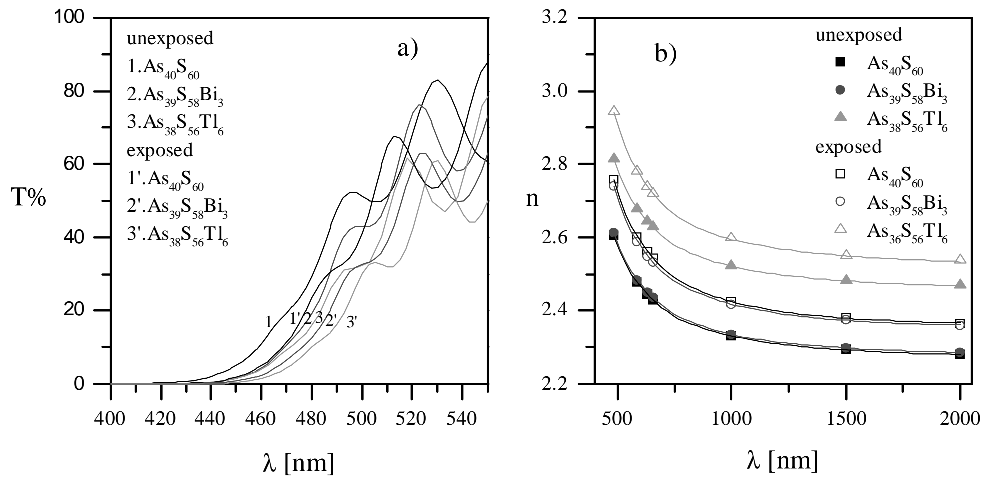

Fig. 3. Optical transmission (a) and refractive index dispersion (b) of thin As-S-Bi(Tl) films vs. wavelength, λ, before and after illumination. Thise compositions are the ones exhibiting the largest light-induced changes in optical properties.

From the transmission measurements we have calculated the refractive index of thin films from the above systems. It was found that the values of n increase for both systems (As-S-Bi and As-S-Tl) and the maximum changes in n were observed for thin layers with the same compositions - $As_{39}S_{58}Bi_3$ (Δn = 0.10) and $As_{38}S_{56}Tl_6$ (Δn = 0.16) (Fig. 3b). At the same time a decrease in the film thickness after exposure to light was found (for the composition $As_{38}S_{56}Tl_6$ Δd = -15 nm). In Table 6 the ellipsometrically determined values of n and d of thin As-S-Bi(Tl) films are shown. The calculated optical constants differ considerably in comparison with those determined by UV-VIS-NIR spectrophotometry for both unexposed and exposed thin films but the composition and exposure dependence was the same.

Table 6. Data for *n* and *d* for unexposed and exposed thin As-S-Bi(Tl) films.

Composition	n unexp	n exp	d unexp [nm]	d exp [nm]
$As_{39}S_{58}Bi_3$	2.477	2.450	1014	978
$As_{38}S_{56}Bi_6$	2.367	2.353	1118	1117
$As_{39}S_{58}Tl_3$	2.367	2.493	1036	1037
$As_{38}S_{56}Tl_6$	2.712	2.832	930	877
$As_{36}S_{54}Tl_{10}$	2.599	2.632	1073	1044

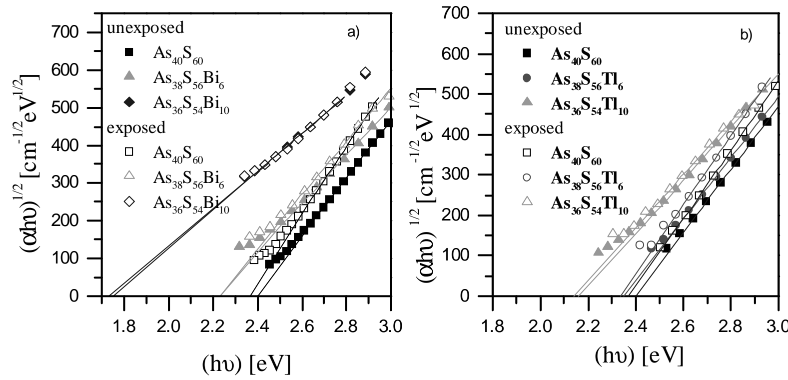

Fig. 4. Optical absorption edge $(\alpha h\nu)^{1/2}$ vs. energy of photon (hν) for unexposed and exposed thin As-S- Bi(Tl) films.

The plots of $(\alpha h\nu)^{1/2}$ vs. hν for unexposed and exposed As-S-Bi films depending on Bi content are shown in Fig. 4a. In the range of high absorption the linear dependence is preserved and it is evident that the absorption edge shifts to lower photon energies as the Bi content increases. The band gap for the unexposed films decreases from E_g = 2.39 eV for $As_{40}S_{60}$ to E_g = 2.06 eV for $As_{36}S_{54}Bi_{10}$). For as-deposited As-S-Tl films the optical band gap decreases to 2.16 eV for thin $As_{36}S_{54}Tl_{10}$ films (Fig. 4b) [20]. At the same time the slope of the absorption coefficient decreases because of a decrease in disordering. The values of *B* decreases from 777 $cm^{-1/2}eV^{11/2}$ for $As_{39}S_{58}Bi_3$ to 563 $cm^{-1/2}eV^{11/2}$ for the composition $As_{36}S_{54}Bi_{10}$. After exposure of thin As-S-Bi(Tl) films, the absorption edge is shifted to longer wavelengths - an effect of photodarkening is observed. The optical band gap decreases for both systems and the largest changes were found for composition $As_{39}S_{58}Bi_3$ - Eg = 0.04 eV (Fig. 4a). The decrease in the band-gap with an increased Bi or Tl content occurs because the latter creates localized states in the bandgap.

3.3. Optical properties of thin Ge-S-Bi(In, Tl) films

Amorphous Ge-containing thin films show irreversible photo- and thermo-bleaching, resulting from exposure to band-gap light and heat treatment, respectively [36-41]. These changes usually could be explained by bond-breaking models but recently the role of oxygen has been taken into account. In our experiments [42] we have studied the photo- induced changes in the optical properties of vacuum deposited Ge-containing films depending on the composition and exposure to light using transmission and reflection me surements. First we have followed out the changes in the optical properties of thin Ge_xS_{100-x} films (a20 ≤ x ≤ 40) (50 and 1000 nm thick). As it was already shown for thin As-S-Ge layers an effect of photobleaching for all of the investigated thin Ge–S films (1000 nm) has been observed (Fig. 5). With increasing of the Ge content the absorption edge shift decreases. The dispersion of refractive index, *n*, vs. wavelength, λ, is shown in Fig. 6. The increase in Ge content leads to a great increase in *n* – from 2.14 for $Ge_{20}S_{80}$ to 2.73 for $Ge_{40}S_{60}$. After exposure to light the values of *n* decrease. It was interesting to calculate the optical constants of very thin films

(50–60 nm thick). The data for the thicknesses calculated with an accuracy of ±1–1.5 nm have been shown in Table 7. The most accurately calculated film thickness was used for determination of the optical constants by double (T, R_f) and (T, R_b) methods, using Newton-Raphson's iterative method [27]. For each of the applied methods for determining the optical constants and the thicknesses, the absolute maximum errors were evaluated [27]. In Table 7, the calculated values of n at λ = 632.8 nm with an accuracy of ± 0.02 using the T, R_f method were compared with the measured ones from the ellipsometric measurements.

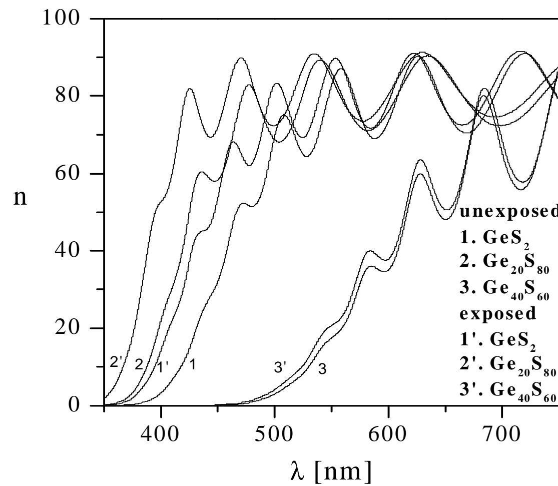

Fig. 5. Photoinduced changes in the transmission of unexpoised and exposed Ge-S layers.

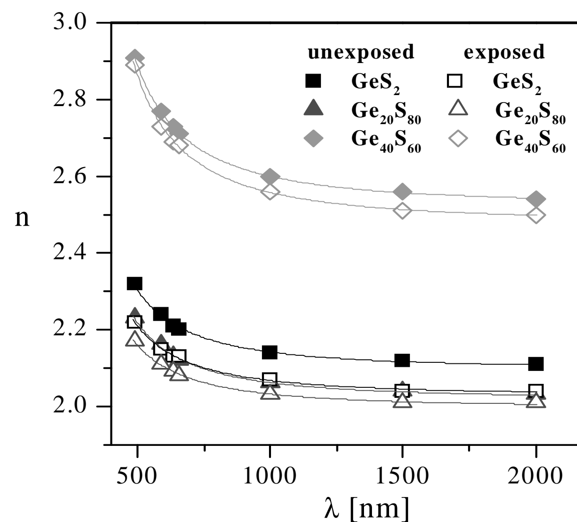

Fig. 6. Refractive index, n, vs. wavelength, λ, of unexposed and exposed Ge-S thin films.

The dependence of n for 50 nm thick Ge_xS_{100-x} films is the same as that for 1000 nm thick layers except the value for he composition $Ge_{40}S_{60}$.

It was found (Fig.7) that the optical band gap decreases from 2.77 eV for thin films with a composition of $Ge_{20}S_{80}$ to a value of 1.75 eV for the composition $Ge_{40}S_{60}$. After exposure to light, the absorption edge shift was to the higher photon energies and an increase of the band gap was observed most probably connected with an increase of the Ge-S bond density and a decrease of the randomness

of the film structure. The highest changes in E_g (ΔE_g = 0.19 eV) were found for the stoichiometric composition GeS_2.

The transmission spectra of as-deposited thin Ge–S–Bi (In, Tl) films showed that the absorption edge was shifted to the longer wavelengths when metals were added to GeS_2.
After exposure to light, the effect of photobleaching typical of all Ge-containing thin films persisted. Photobleaching was most pronounced in the compositions $(GeS_2)_{0..93}Bi_{0.07}$ ($\Delta\lambda$ = - 20 nm at T = 20 %) and $Ge_{32}S_{64}Tl_4$. The values of refractive indices for unexposed Ge-S-Me layers calculated from the transmission measurements increased with increasing of Me content (from 2.16 for GeS_2 to 2.69, 2.75 and 2.33 for $Ge_{30}S_{60}Bi$, $(In, Tl)_{10}$, respectively at λ = 632.8 nm. The incorporation of Bi, Tl and In in unexposed GeS_2 layer leads to a shift of the absorption edge to the lower photon energies, i.e. to a decrease of the optical band gap, E_g , (from 2.52 eV for GeS_2 to 1.88 eV for $Ge_{30}S_{60}Bi_{10}$,and to 1.93 and 2.34 eV for $Ge_{30}S_{60}In_{10}$ and $Ge_{30}S_{60}Tl_{10}$, respectively. This effect might be attributed to the creation of localized states in the band-gaps.

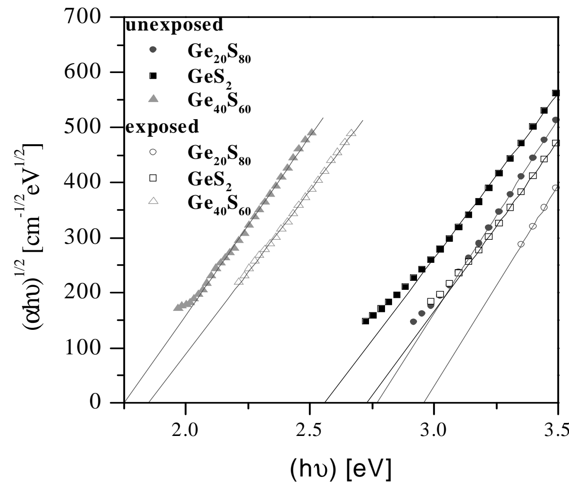

Fig. 7. Optical absorption edge $(\alpha h\nu)^{1/2}$ vs. photon energy ($h\nu$) for unexposed and exposed thin Ge-S films .

Table 7. Comparison between the values for *d* and *n* for thin Ge_xS_{100-x} films obtained by spectrophotometry and ellipsometry measurements at λ = 632.8 nm.

Composition	(T, R, R_m) method		Ellipsometric		(T, R) method		Ellipsometric	
	d_{unexp} [nm]	d_{exp} [nm]	d_{unexp} [nm]	d_{exp} [nm]	n_{unexp}	n_{exp}	n_{unexp}	n_{exp}
GeS_2	53	54	53.0	54.4	2.16	2.05	2.144	2.056
$Ge_{20}S_{80}$	52	50	51.5	53.5	2.07	2.06	2.094	2.049
$Ge_{40}S_{60}$	43	43	46.2	46.4	2.67	2.61	2.616	2.587

After exposure (the exposure time to saturation was experimentally established for any composition) *n* decreases for all ternary compositions and Δn passed through a maximum at the above mentioned compositions. The results obtained from ellipsometric measurements (Table 8) showed the same dependence of *n* for unexposed and exposed films on Me content in the

GeS_2. The highest changes of the band gap, ΔEg, after exposure was estimated to be for a metal content about 4 at.%.

Table 8. Data fo rΔd and refractive index, n, calculated from ellipsometric measurements (at λ = 633 nm) of thin unexposed and exposed films from the systems Ge-S-Bi and Ge-S-Tl, deposited with a residue in the boat.

Composition	$n_{unexp.}$	n_{exp}	Δn	Δd[nm]
GeS_2	2.160	2.132	-0.03	+46
$Ge_{32}S_{64}Bi_4$	2.195	2.182	-0.01	+10
$Ge_{30}S_{60}Bi_{10}$	2.732	2.736	0	+ 2
$Ge_{32}S_{64}Tl_4$	2.221	2.180	-0.04	+38
$Ge_{31}S_{63}Tl_6$	2.360	2.340	-0.02	+ 5
$Ge_{30}S_{60}Tl_{10}$	2.403	2.380	-0.02	+43
$Ge_{32}S_{64}In_4$	2.200	2.140	-0.06	+19
$Ge_{28}S_{66}In_6$	2.723	2.713	-0.01	+ 5
$Ge_{30}S_{60}In_{10}$	2.726	2.716	-0.01	+ 1

The values of *B* (see equation (1)) for as-deposited Ge-S-Bi tin films decrease with increasing the Bi content in the coatings (from 421 $cm^{-1/2}eV^{-1/2}$ for $Ge_{32}S_{64}Bi_4$ to 220 $cm^{-1/2}eV^{-1/2}$ for $Ge_{30}S_{60}Bi_{10}$. That means that the structural disorder was increased and new localized states in the band-gap are created. The calculated values of *B* for the system Ge-S-Tl passed through a minimum for the composition $Ge_{32}S_{64}Tl_4$. It is known that there are numerous ternary compounds between elements Ge, S and Tl – Tl_4GeS_4, $Tl_2Ge_2S_5$, $Tl_2Ge_2S_4$ and $TlGeS_3$ giving many possibilities for different combinations between the existing bonds Ge-S, Ge-Ge, S-S, Tl-S, Ge-Tl. More details from the IR experiments will be given elsewhere.

3.4. Photoinduced changes in the dissolution rate of thin chalcogenide films

The practical utilization of the As-S films as inorganic photoresists is based on the presence of difference in the dissolution rates of the exposed and unexposed areas of the samples and a secure protection during etching of the chromium coating in the process of fabrication of the metal photomasks. There are numerous factors that influence the dissolution rate of the chalcogenide layer: deposition rate, evaporation temperature, substrate temperature layer composition, exposure conditions, solvent type, pH, concentration and the temperature of the solvent system, additives of inorganic salts and surfactants in the alkaline solutions. The dependence of all these factors on the selectivity of As-S thin films ($\gamma = V_{exp}/V_{unexp}$, where V_{exp} is the dissolution rate of the exposed films and V_{unexp} - the dissolution rate of unexposed films) was studied in details [28, 43-50], We have found that the optimal concentrations of the solvents were - 100 g/l for K_2CO_3 (pH=12.4), 50 g/l for Na_3PO_4 (pH=12.35) and 20 g/l dimethylamine. Fig. 8 shows the dependence of the dissolution rates of As_2S_3 on pH of a solution of 100 g/l K_2CO_3 for two rates of deposition. It is seen that pH influences considerably on the dissolution rate of the exposed film areas and the maximum value of γ being obtained at pH 11.6-12.0. Using the solvent concentrations defined above, the change of γ depending on the deposition rate (temperature of evaporation) was studied. It was observed that the maximum value of γ is obtained when the deposition rate was about 3-4 Å/s. It was found that the selective solubility of the chalcogenide layers depends very strongly on the arsenic content in the coatings (Table 9).

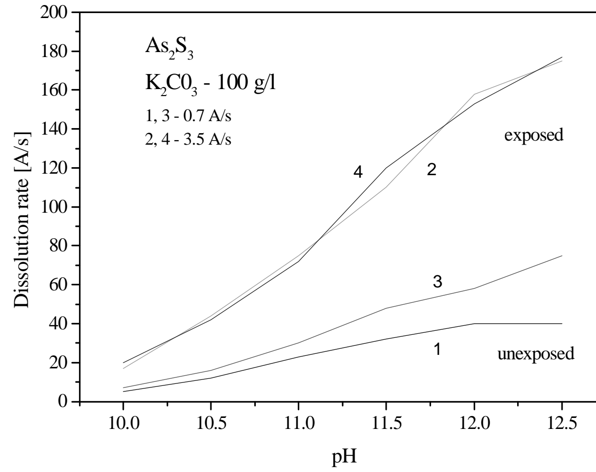

Fig. 8. Dependence of the dissolution rates of As_2S_3 films on pH of a solution of 100 g/l K_2CO_3 for two different deposition rates.

Table 9. Experimental values of V_{unexp}, V_{exp} and γ for As_xS_{100-x} ($33 \le x \le 45$) thin films.

Solution / Contents	20 g/l Dimethylamine			100 g/l K_2CO_3			100g/l K_2CO_3 with surf		
	V_{exp} Å/s	V_{unexp} Å/s	γ	V_{exp} Å/s	V_{unexp} Å/s	γ	V_{exp} Å/s	V_{unexp} Å/s	γ
$As_{33}S_{67}$	1250	400	3.1	200	100	2.0	180	20.00	9.0
$As_{38}S_{62}$	400	100	4.0	135	60	2.3	150	13.00	11.5
$As_{40}S_{60}$	350	53	6.6	100	20	5.0	95	3.50	27.0
$As_{42}S_{58}$	250	25	10.0	100	7	15.7	35	0.90	43.8
$As_{45}S_{55}$	55	4	13.8	60	3	20.0	15	0.25	60.0

The arsenic content was ascertained iodometrically and the results are that in the bulk material, in the material remaining in the crucible after evaporation and in the thin films it does not exceed 0.3 wt.% [47]. The comparison of the dissolution rates shows that small variations in the film composition lead to considerable changes in the dissolution rates in all alkaline solutions studied. The arsenic-enriched layers exhibit greater selectivity (γ). This effect is even pronounced if the developer contains a surfactant [45]. Obviously, the adsorption of the surfactants used is greater on unexposed layers with an increased As content. This process of adsorption is possible only if "wrong" valency bonds are presented between identical atoms or, to put it more precisely, the irreversible surfactant adsorption is realized probably by the As-As bonds whose number grows with the increase of the arsenic content in the samples. Thin films with a composition of $As_{42}S_{58}$ or $As_{45}S_{55}$ may be used as an inorganic photoresist reproducing precisely details with an edge width below 0.1 μm. Unfortunately, the sensitivity of the photolithographic material decreases at higher arsenic content in the films, i.e. longer exposure is needed (up to 50 %). That's why, the composition $As_{42}S_{58}$ is more suitable for photomasks because at the same sensitivity as $As_{40}S_{60}$, its selectivity is higher.

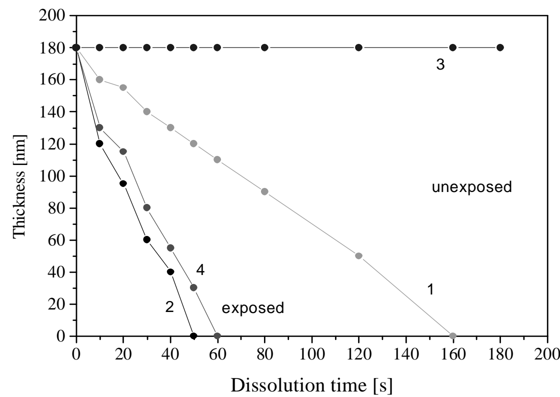

Fig. 9. Data for the thickness of unexposed (1, 3) and exposed (2, 4) As_2S_3 layers *vs.* time of dissolution without (1, 2) and in the presence (3, 4) of surfactant in the solution.

The kinetics of chemical dissolution of thin films of chalcogenide glasses can be helpful for determining the possibilities for their use as an inorganic photoresist as well as to elucidate the mechanism of glass-solvent interaction. Table 9 and Table 10 (where data for the dissolution rates and the selectivity, γ, of thin As-S films in the alkaline solvent, described in [46, 47] are presented) show that the dissolution is strongly influenced by the presence of some surfactants. Their action makes possible the practical application of As_2S_3 layers as an inorganic photoresist. Studying the temperature dependence of the dissolution process we were able to give an explanation of this phenomenon [49]. Fig. 9 follows the changes in the thickness of unexposed (1, 2) and exposed (3, 4) thin As_2S_3 films with the time of dissolution. The difference between the two rates becomes much greater when a surfactant is added to the solvent (3, 4). For all temperatures studied (in the range of 15-45°), lg V_{diss} of the exposed arsenic sulfide layers with and without surfactants at different temperatures increases linearly with pH of the solution. From the temperature dependence of the rate of dissolution the activation energy E_a of the process was determined. Calculated by the least squares method, the values of E_a obtained for the exposed parts, at any pH were E_a=99 kJ/mol (with surfactant) and 91 kJ/mol (without a surfactant). Taking into account the accuracy of the experiment - 10%) it can be assumed that the activation energy of the process of dissolution of the exposed parts does not depend on the presence or absence of surfactants. The activation energy of dissolution of unexposed layers without surfactants could be determined only in the interval pH 11.5 and t 30°C, and was found to be about 80 kJ/mol.

Table 10. Data for the dissolution rates and γ for thin As-S films obtained in solvent containig 100 g/l Na_2CO_3, 150g/l Na_3PO_4 without and with surfactant at pH = 11.4.

Solution / Contents	$Na_2CO_3 + Na_3PO_4$			$Na_2CO_3 + Na_3PO_4$ with surfactant		
	V_{exp} Å/s	V_{unexp} Å/s	γ	V_{exp} Å/s	V_{unexp} Å/s	γ
$As_{33}S_{67}$	215	215	1.0	240	235	1.0
$As_{38}S_{62}$	240	180	1.3	260	125	2.1
$As_{40}S_{60}$	370	70	5.3	335	15	22.3
$As_{42}S_{58}$	165	20	8.3	195	2	97.5
$As_{45}S_{55}$	95	15	6.3	95	2	47.5

When a surfactant is presented, however, the unexposed parts dissolve extremely slowly and at $pH < 12.0$ and $t < 30°C$ the dissolution energy remains practically zero and E_a cannot be determined. At the range $12.0 < pH \leq 12.8$ and $t > 30$ °C the activation energy was found to be about 160 kJ/mol and finally for $pH \geq 12.8$ and $t \geq 30$ °C it was 84 kJ/mol.

As a result from our investigations an inorganic photoresist was developed and more than 20 years it is utilized for many photolithographic purposes. Many of the results published were confirmed and our ideas were extended by other scientists [9, 51-54] who developed new materials using new etching solvents.

3.5. Dry etching of thin chalcogenide layers

The process of dry plasma etching is widely applied in microelectronics. Compared with the conventional wet etching process it has some advantages because it is dry, clean and provides higher resolution of the photolithographic materials. The first result on the etching of Ag-photodoped As_2S_3 was published in 1978 [55]. The maximum ratio between the etching rates of doped and undoped parts of the layers was 1.8 in CF_4 plasma. Using the same plasma for differential etching of illuminated and unilluminated areas of a spin coated As_2S_3 films it was found the rates of dry-etching of the two parts are 230 and 92 Å/s, respectively [56].

We have used a modified commercial vacuum equipment HZM-4 (Germany) for etching thin chalcogenide layers with different compositions. The diode electrode configuration was connected to a 2.5 MHz rf power supply. The rf power density was varied in the range of 50-350 $mW.cm^{-2}$. Most often the experiments were performed at a pressure about 8 Pa and a power density of 130 $mW.cm^{-2}$. Table 10 shows some data obtained for chemical dry etching of unexposed and exposed thin chalcogenide films from Ge-S-As(Bi) system. It seems that the etching rate of unexposed thin layers depends very strongly on the thin film composition. Adding small quantities of Bi in GeS_2 layers they become completely unetchable in CCl_2F_2 plasma. That means we can use the photodoped GeS_2 with Bi as a mask for obtaining deep etched structures in chalcogenide bulks or thin layered substrate.
We have found that the etch rate of thin films decreases with increasing the etching time probably as a result of the products of the chemical reaction taking place on the film surface. The etching rates depend strongly on the power density supplied on the samples. This process will be studied more carefully because it gives a possibility for practical utilization of chalcogenide glasses as an inorganic photoresist.

Table 11. Chemical dry etching rates of unexposed and exposed thin chalcogenide films: etching time – 180 s; CCl_2F_2 plasma - rf power density-130$mW.cm^{-2}$.

Composition	Unexposed Å/s	Exposed Å/s
$Ge_{33}S_{67}$	15.6	6.7
$Ge_{28}S_{66}Bi_6$	0.9	1.1
$Ge_{30}S_{60}Bi_{10}$	0.4	1.6
$As_{40}S_{60}$	36.7	27.5
$As_{30}Ge_{10}S_{60}$	65.0	18.3
$As_{20}Ge_{20}S_{60}$	51.7	18.3

3.6. ESCA analysis of thin As_2S_3 films

Some papers exist in the literature on the spectroscopic studies of chalcogenide glassy systems [57-59]. It is shown that the bonding state between the constituent elements in Ge-Se alloys

varies with the compositional ratio of the elements. Ultraviolet irradiation of arsenic sulfide surface in the presence of oxygen results in photoinduced changes of chemical composition, which are accompanied by selective oxidation of the surface of the As constituent. We have studied the changes in stoichiometry of thin As_2S_3 films deposited on Cr undercoated glass substrates after exposure to light. Our spectra (Table 10) show that illumination results in higher binding energies in comparison of those of unexposed sample, i.e. a shift of the As 3d peak from 42.8 eV for an unexposed sample to 43.1 eV for an exposed one is observed; as well as a shift of S 2p from 161.9 eV to 162.2 eV. The shift of the As 3d peak is 0.2-0.4 eV, which is considerably less than that observed in Ref. 59.

Comparison of the As 3d to S 2p normalized peak area ratio (As/S for unexposed samples with the same ration for exposed films shows a decrease by 0.1 for the exposed ones. This change of the As/S ratio shows a change in stoichiometry of the surface of As_2S_3 layers. The conclusion which could be drawn is that as a result of laser irradiation, photo-induced oxidation of arsenic occurs in the surface layer of thin films, i.e. As_2O_3 is formed. It probably desorbs at relatively low temperatures. The irradiation results in a decrease in intensity of the O 1s peak, which is one more proof of the photo-induced oxidation of arsenic and desorption of arsenic oxide. In depth of As_2S_3 layers, no presence of oxygen is registered. All this confirms the statement that the above effects have a surface character.

Table 11. XPS data on the surface of thin As_2S_3 films.

Sample No	As 3d - BE (eV)		S 2p - BE (eV)		O 1s - BE (eV)	
	unexposed	exposed	Unexposed	Exposed	unexposed	exposed
1	42.6	43.1	161.9	162.2	530.9	532.5
2	42.8	43.1	161.9	162.2	531.2	532.1
3	42.9	43.1	161.9	162.2	531.3	532.0

3.7. Applications

There are many current and potential applications of photoinduced effects in chalcogenide glasses and thin films reviewed in several papers [3, 5, 9, 60]. In the present work we will give data for some materials fabricated in the Central laboratory of photoprocesses which are based on changes of transmittance, reflectance and index of refraction as well as the dissolution of thin chalcogenid layers. Using the effect of photo-induced metal diffusion of Ag into As_2S_3 thin films after irradiation with light with energy comparable to that of the bandgap of chalcogenide several photographic materials have been developed: photographic material for flexible printed plates, photographic material for offset printing and plates with high resolution [61-63]. The principal scheme of their processing is shown in Fig.10. After exposition through a mask and dissolution of the products of the reaction and the unreacted As_2S_3 the silver nuclei remaining on the substrate can be intensified by a physical developer or by palladium and chemical or galvanic copper deposition. In the first case a glass substrate coated with chromium [64, 65] was used. The plates obtained have a resolution 1500-2000 lines/mm, maximum density over 2.0 and light sensitivity comparable to that of "Shipley AZ-1350" photoresist. They can be used for project and contact printing in microelectronics.

When the system is deposited on flexible polyester substrate with organic overcoating, a photographic material for preparation of flexible conductors for electronics is obtained. After copper deposition electroconductive tyres, several microns thick are obtained with good adhesion to the substrate (1000-1500 g/cm^2). The resolution of the offset printing elements (a negative system) was 120 lines/mm with a sensitivity comparable to that of the diazocompounds and endured up to 30000 copies.

As already shown, even without surfactant the dissolution rate of the exposed As_2S_3 thin films is greater than the unexposed. However the difference between the two rates becomes much greater if

the dissolution proceeds with surfactants. This makes possible the practical application of arsenic sulfide layers as inorganic photoresist.

A new technology for production of metal images with micron and submicron sizes onto glass substrates has been developed in our laboratory. It includes the preparation of clean substrates, vacuum deposition of inorganic photoresist and photolithographic processing. The basic element of the new technology is the inorganic photoresist developed in CLF. It represents vacuum evaporated thin film of As_2S_3 (100 nm thick) which when treated in an alkaline solution in the presence of some dyes exhibits high selectivity and considerable stability in acid etching chromium solutions. The small film thickness and its amorphous structure allow reproduction of details with line width of 0.35 μm at optical reproduction and 0.1 μm on exposure with electrons. Besides, the permissible exposure tolerance (± 30%) and processing time (±100 %) noticeably surpass those of conventional photoresists used in practice. The quick processing of the new photolithographic material and its good adhesion to chromium, nickel, glass, aluminium, TiO_2, etc. makes it especially suitable for mass copying of precision scales, gratings for circular and linear transducers. The material is appropriate for preparing diffraction optical elements with parameters having no analogy in world practice. Compared to the conventional systems the new technology decreases substantially the product price and allows to reproduce macro as well as microdetails at equal conditions of exposure and processing.

4. Discussion

The films of chalcogenide glasses represent inorganic polymers with a specific branched polymer structure. According to some authors, the as-evaporated As_xS_{100-x} layers (for $x \leq 40$) are a heterogeneous mixture of structural units of the type As_2S_3, As_4S_3, As_4S_4, As_4S_8, As_4, S_8 and contain some homeopolar bonds (As-As, S-S). The presence of As_4S_4 is responsible for the appearance of peaks at 375 and 336 cm^{-1} in the infrared spectra, and the AsS_3 pyramids for the peak at 310 cm^{-1}. These values are very close to those cited in literature [66-68].

On illumination, polymer destructive changes occur leading to the weakening of some bonds and to strengthening of others [50]. The existence of structural changes in such vitreous chalcogenide films on illumination is supported by X-ray investigations as well as by changes in the physico-chemical properties, as for example, microhardness and temperature of softening.

Our experiments, performed at various evaporation and substrate temperatures, showed that the dissolution rate of the exposed films remains almost unchanged, whereas the evaporation temperature influences the dissolution rate of the unexposed films, and hence γ.

The increase in the deposition rate results in a decrease in the dissolution rate of the unexposed films and an increase in γ. Obviously, the exposure brings the system into one and the same state. That is why, neither the evaporation temperature, nor the type of sulfide has any effect on the dissolution rate of the unexposed areas of the film. The dissolution of the layers containing As_4S_4 units (or As-As bonds) is slow with higher activation energy, and the dissolution rate of layers without these units is higher. These units are not presented in samples with overstoichiometric sulfure ($x \leq 40$) because of another dissolution mechanism.

The irreversible change occuring after exposure of as-deposited films are accompanied by a density increase of the As-S bonds, i.e. a photopolymerization process of As_4S_6 molecules. This leads to an increase in refractive index and dissolution rate, a decrease in activation energy of the process, and considerable changes in the absorption peaks at 375 and 308 cm^{-1} obtained by infrared spectroscopy [50].

It was suggested that the addition of Tl_2S to As_2S_3 glasses breaks some As-S-As bridges in order to form new bonds between electrically charged ions. The existence of photo-induced structural changes in such chalcogenide films is supported by changes in their optical properties. The addition of Tl or Bi to arsenious sulfide leads to the increase of the refractive index and decrease of E_g and to the creation of localized states in the band-gap. The same is the effect with the incorporation of these metals in germanium sulfide. The localized states of amorphous are mainly influenced by the microscale disorder. Thus, the photobleaching of Ge-S thin films may be explained only by the increase of the microscale disorder by illumination. For better understanding the nature of the photostructural changes we need some IR and Raman investigations of ternary glass compositions.

5. Conclusions

The conditions for synthesizing chalcogenide glasses with specific compositions have been established. The results from the X-ray microanalysis performed showed that the compositions of bulk samples are very close to the expected compositions. The bulk samples were subjected to X-ray and electron diffraction analysis, which confirmed that only amorphous phase was identified. The compositions $As_{45}S_{55}$ and those from the system Ge-S-In were an exception, containing traces of a crystalline phase, molecules of As_4S_4 and crystal $\alpha - GeS_2$ phase.

The method of evaporation influences considerably the properties of thin chalcogenide films. The struture and the composition in the depth of the layer as well as the optical properties and the dissolution rate depend on the temperature of evaporation (the deposition rate). The addition of surfactants lowers considerably the dissolution rate of the unexposed areas of the As_2S_3 films and makes their processing especially sensitive to pH of the solution. The dissolution rate, activation energy of dissolution and optical properties of thin As-S films depend strongly on the As content in the coatings. Most suitable for developing an inorganic photoresist are the films with composition $As_{42}S_{58}$, since they exhibit the highest selective solubility, widest limits of processing, a sensitivity close to that of organic resists, and good reproducibility.

The assumption for a selective adsorption of surfactants on the unexposed samples finds its explanation in some observations by other authors. Berkes et al. [69] established that even in stoichiometric amorphous chalcogenide layers there are always bonds between identical atoms, which are broken on exposure. Strom and Martin [68] examined the IR-spectra of deposited layers of arsenic sulfide and established the presence of As-S bonds. They also proved that the latter are broken on exposure, the disorder decreases and normal heteropolar bonds As-S are formed.

It seems that the chemisorption of the surfactants is possible only in the presence of such unusual valent bonds between identical atoms in As_2S_3 which are destructed on exposure. The selective adsorption of the surfactant probably occurs at the As-As bonds. Vacuum deposited layers of another chalcogenides, not containing As, do not show selective adsorption of surfactant and their dissolution rate is not influenced by its presence.

The transmittance measurements of the chalcogenide thin films showed that for all As-containing coatings the absorption edge was shifted to the longer wavelengths (an effect of photodarkening) while for all Ge-containing layers it was shifted to the shorter wavelengths (an effect of photobleaching). The highest values of the shift was as followed: $As_{42}S_{58}$ - $\Delta\lambda$ = 40-50 nm (at T = 30 %); $As_{38}S_{68}Tl_3$ - $\Delta\lambda$ = 20-25 nm (at T = 30 %); $As_{10}Ge_{30}S_{60}$ - $\Delta\lambda$ = 25-40 nm (at T = 30 %); $Ge_{31}S_{63}Tl_6$ - $\Delta\lambda$ = 50-60 nm (at T = 30 %);

The refractive indices have been calculated and limits of their variation have been determined in all thin films investigated. With the increase in arsenic content of the thin Ge-S-As layers, the refractive index of unexposed films increases and its change Δn decreases after illumination. For the most precise determination of the optical constants it is necessary to use both spectrophotometric and ellipsometric measurements and to take account of the homogeneity of the layers because very often their compositions is changed in the volume of the films.

The preliminary experiments on the process of dry etching of the ternary chalcogenide layers showed that it is possible to receive structures in some of them using CCl_2F_2 plasma.

The selective dissolution of thin As-S films depends on the type, concentration and pH of the alkaline solutions, passing through a maximum for particular values. The addition of surfactants lowers considerably the dissolution rate of unexposed areas of the films and makes their processing especially critical to pH of the solution. The most suitable for photolithographic application are thin $As_{42}S_{58}$ films because of their very high selective solubility. The selectivity of wet dissolution of Ge-containing chalcogenide layers in alkaline solvents is not very high. As an exception we could note that after exposure to light thin $Ge_{28}S_{66}Bi_6$ films became insoluble.

References

[1] P. J. S. Ewen, A. E. Owen, High Performance Glasses, Blackie, London (1992), p. 287.
[2] G. Pfeiffer, M. A. Paesler, S. C. Agarwal, J. Non-Cryst. Solids **130**, 111 (1991).

[3] A. M. Andriesh, V.V. Ponomar, V. L. Smirnov, A. V. Mironas, Sov. J. Quantum Electronics **16**, 721 (1986).
[4] Mutsuo Takenga, Masanari Mikoda, in: Y. Hamakawa (Ed.), Optical Memories, Amorphous Semiconductor Technologies & Devices **16**, Ohmsha LTD(1984), p. 266.
[5] S. Elliott, Chalcogenide Glasses, Chapter 7, Mat. Sci. Tech. **9** (1991), p. 376.
[6] S. R. Elliott, J. Non-Cryst Solids **81**, 71 (1986).
[7] K. Tanaka, Rev. Solid State Sci. **4**, 641 (1990).
[8] K. Shimakawa, A. Kolobov, S.R. Elliott, Advances in Physics **44**, 475 (1995).
[9] M. Frumar, Z. Polak, Z. Cernosek, M. Vlcek, B. Frumarova, Photoinduced Effects in Amorphous Chalcogenides in Physics and Applications of Non-Crystalline Semiconductors in Optoelectronics, Kluwer Academic Publishers (1997), p. 123.
[10] K. Tanaka Thin Solid Films **66**, 271 (1986).
[11] E. Marquez, J. Ramirez-Malo, P. Villares, R. Jimenez-Garay, P.J.S. Ewen, A.E. Owen, J. Phys. D: Appl. Phys. **25,** 535 (1992).
[12] M. Kotkata, H.T. El-Shair, M.A. Afifi, M.M. Abdel-Aziz, J. Phys. D: Appl. Phys. **27,** 623 (1994).
[13] E. Marquez, A.M. Bernal-Oliva, J.M. Gonzalez-Leal, R. Pireto-Alcon, R. Jimenes-Garay, J. Non-Cryst. Sol. **222**, 250 (1997).
[14] E. Marquez, P. Nagels, J.M. Gonzalez-Leal, A.M. Bernal-Oliva, E. Sleeckx, R. Callaerts, Vacuum **52**, 55 (1999).
[15] Y. Laaziz, A. Bennouna, N. Chahboun, A. Outzourhit, E. L. Ameziane, Thin Solid Films **372**, 149 (2000).
[16] R. Swanepoel, J.Phys. E: Sci. Instrum. **16**, 1214 (1983).
[17] U. Borisova, Chimija stekloobraznych poluprovodnikov, Verl. Leningr. Univ., 1972, p.107.
[18] W.Vogel, Glas-chemie, VEB Deutscher Verlag fur Grundstoffindustrie, Leipzig (1979), p. 59.
[19] K. Petkov, R. Todorov, D. Kozhuharova, Proc. 9th Int. School on Condensed Matter Physics, 9-13 September, 1996, Varna, Bulgaria.
[20] K. Petkov, R. Todorov, Tz. Iliev, Proc. 10th Int. School on Condensed Matter Physics, 1-4 September 1998, Varna, Bulgaria.
[21] K. Petkov, B. Dinev, J. Mater. Sci **29**, 468 (1994).
[22] I. Konstantinov, Private communication (1989).
[23] J. Tauc, Amorphous and liquid semiconductors (Plenum Press) New York (1974).
[24] V. Panayotov, I. Konstantinov, Bulg. Chem. Commun. **26**, 612 (1993).
[25] R. Todorov, Tz. Babeva and K. Petkov, Proc. 11th ISCMP, 1-4 September 2000, Varna, Bulgaria.
[26] F. Abeles, M. Theye, Surf. Sci. **5**, 325 (1966).
[27] I. Konstantinov, Tz. Babeva, S. Kitova, Appl. Opt. **37**, 4260 (1998).
[28] K. Petkov, V. Fedorov, Comptes rendus de l'Acad. Bulg. Sci. **35**, 921 (1982).
[29] K. Petkov, V. Krastev, Tz. Marinova, Surface and Interface Analysis **22**, 205 (1994).
[30] J. Ramirez-Malo, E. Marquez, P. Villares, R. Jimenez-Garay, Mater. Let. **17** (1993) 327.
[31] J.M. Gonzalez-Leal, E. Marquez, A.M. Bernal-Oliva, J.J. Ruiz-Perez, R. Jimenez-Garay, Thin Solid Films **317,** 323 (1998).
[32] N. F. Mott, E. A. Davis, Electron Processes in Non-Crystalline Materials, Mir, Moskow (1982), p. 198.
[33] E. Vateva, P. Minkov, E. Skordeva, D. Arsova, M. Nikiforova, J. Non-Cryst. Solids **90**, 481 (1987).
[34] K. Tanaka, Phys. Rev. **B39**, 1270 (1989).
[35] R. Todorov, K. Petkov, J. Optoelectronics and Adv. Mater. **3**, 311 (2001).
[36] L. Tichy, H. Ticha, M. Vlcek, J. Klikorka, K. Jurek, J. Mater. Sci. Lett. **5**, 1125 (1986).
[37] L. Tichy, A. Triska, H. Ticha, M. Frumar, Phil. Mag. **B54**, 219 (1986).
[38] L. Tichy, H. Ticha, K. Handlir, K. Jurek, Phil. Mag. Lett. **58**, 233 (1988).
[39] L. Tichy, H. Ticha, K. Handlir, K. Jurek, J. Non-Cryst. Solids **101**, 223 (1988).
[40] Z. G. Ivanova, V. S. Vassilev, J. Non-Cryst. Solids **192&193**, 439 (1995).
[41] E. Vateva, E. Skordeva, D. Arsova. Phil. Mag. B **67,** 225 (1993).
[42] R. Todorov, Tz. Iliev, K. Petkov, to be published.
[43] K. Petkov, J. Signal AM **12**, 53 (1984).

[44] K. Petkov, Bulg. J. Phys. **12**, 519 (1985).
[45] I. Konstantinov, B. Mednikarov, M. Sachatchieva, A. Buroff, U.S. Patent 4 499 173 (12.02.1985).
[46] B. Mednikarov, Solid State Technol. **27**, 177 (1984).
[47] K. Petkov, M. Sachatchieva, J. Dikova, J. Non-Cryst. Solids **101**, 37 (1988).
[48] K. Petkov, Bulg. Chem. Commun. **26**, 482 (1993).
[49] K. Petkov, M. Sachatchieva, N. Malinowski, J. Non-Cryst. Solids **85**, 309 (1996).
[50] K. Petkov, M. Vlhek, M. Frumar, J. Mater. Sci. **27,** 3281 (1992).
[51] M. Vlcek, M. Frumar, M. Kubovy, V. Nevsimilova, J. Non-Cryst. Solids **137&138**, 1035 (1991).
[52] M. Frumar, M. Cvikal, M. Vlcek, T. Wagner, J. Non-Cryst. Solids **164-166**, 1243 (1993).
[53] M. Vlcek, J. Prokop, M. Frumar, Int. J. Electronics **77**, 969 (1994).
[54] M. Frumar, Z. Polak, Z. Cernosek, B. Frumarova, T. Wagner, Chem. Papers **51**, 304 (1997).
[55] M. S. Chang, J. J. Chen, Appl. Phys. Lett. **33**, 892 (1978).
[56] E. Hajto, R. E. Belford, P. J. S. Ewen, A. E. Owen, J. Non-Cryst. Solids **115**, 129 (1989).
[57] T. Uneo, A. Odajima, Jpn. J. Appl. Phys. **19**, L519 (1980).
[58] H. Kawamura, M. Matsumura, S. Ushioda, J. Non-Cryst. Solids **35/36**, 1215 (1980).
[59] A. V. Kolobov, Jas P. S. Badyal, R. M. Lambert, Surf. Sci. **222**, L819 (1989).
[60] K. Petkov, Proc. 11th Conference on Glass and Ceramics, Varna, 25-27.10.1993, "Marin Drinov" Acad. Publishing House, Sofia, 1994, p. 49.
[61] A. Buroff, PhD Thesis (1982).
[62] A. Buroff, R. Stoycheva-Topalova, Bulg. Chem. Commun. **26**, 566 (1993).
[63] R. Stoycheva-Topalova, J. Photogr. Sci. **31**, 45 (1983).
[64] R. Stoycheva, K. Petkov, A. Buroff, J. Signal Am. **8**, 347 (1980).
[65] K. Petkov, R. Stoycheva, J. Signal AM **9**, 135 (1981).
[66] A. Bertoluzza, C. Haymano, P. Monti, G. Semerano, J. Non-Cryst. Solids **29**, 49 (1978).
[67] N. Tohge, M. Kimoto, T. Minami, M. Tanaka, Jpn. J. Appl. Phys. **19**, 213 (1980).
[68] U. Strom, T. P. Martin, Solid State Commun. **29,** 527 (1979).
[69] J. S. Berkes, S. W. Ing, W.J. Hillegas, J. Appl. Phys. **42,** 4908 (1971).